RESEARCH PAPERS

Acta Cryst. (1998). D**54**, 1207–1215

Biochemical and Crystallographic Characterization of Homologous Non-peptidic Thrombin Inhibitors Having Alternate Binding Modes

Corey L. Strickland,[a] John. M. Fevig,[b] Robert A. Galemmo Jr,[b] Brian L. Wells,[b] Charles A. Kettner[b] and Patricia C. Weber[a]*

[a]*Schering-Plough Research Institute, 2015 Galloping Hill Road K15-3-3855, Kenilworth, NJ 07033-0539, USA, and* [b]*The DuPont Merck Pharmaceutical Company, PO Box 80500, Wilmington DE 19880-0500, USA.*
E-mail: patricia.weber@spcorp.com

(*Received 22 September 1997; accepted 17 December 1997*)

Abstract

The X-ray crystallographic structure of [*N*-(3-phenylpropionyl)-*N*-(phenethyl)]-Gly-boroLys-OH (HPBK, $K_i = 0.42$ n*M*, crystallographic *R* factor to 1.8 Å resolution, 19.6%) complexed with human α-thrombin shows that the boron adopts a tetrahedral geometry and is covalently bonded to the active serine, Ser195. The HPBK phenethyl aromatic ring forms an edge-to-face interaction with the indole side chain of Trp215. Four HPBK analogs containing either electron-withdrawing or electron-donating substitutents at the 3′ position of the phenethyl ring were synthesized in an attempt to modulate ligand affinity by inductive stabilization of the edge-to-face interaction. Refined crystallographic structures of the trifluoromethyl (K_i = 0.37 n*M*, crystallographic *R* factor to 2.0 Å resolution = 18.7%), fluoro (K_i = 0.60; *R* factor to 2.3 Å resolution = 18.4%), methoxy (K_i = 0.91 n*M*, *R* factor to 2.2 Å resolution = 19.8%) and methyl (K_i = 0.20 n*M*, *R* factor to 2.5 Å resolution = 16.9%) HPBK analogs complexed with thrombin revealed two binding modes for the closely related compounds. A less than 1.5-fold variation in affinity was observed for analogs (trifluoromethyl-HPBK and fluoro-HPBK) binding with the edge-to-face interaction. The slight inductive modulation is consistent with the overall weak nature of the edge-to-face interaction. Owing to an unexpected rotation of the phenethyl aromatic ring, the 3′ substituent of two analogs, methoxy-HPBK and methyl-HPBK, made direct contact with the Trp215 indole side chain. Increased affinity of the 3′ methyl analog is attributed to favorable interactions between the methyl group and the Trp215 indole ring. Differences in inhibitor, thrombin and solvent structure are discussed in detail. These results demonstrate the subtle interplay of weak forces that determine the equilibrium binding orientation of inhibitor, solvent and protein.

1. Introduction

The perpendicular arrangement of aromatic rings is a recurrent feature contributing to the stabilization of protein structures (Burley & Petsko, 1985; Hunter *et al.*, 1991; Singh & Thornton, 1985) and protein–ligand complexes (Burley *et al.*, 1987; De Vos *et al.*, 1988; Ishida *et al.*, 1993). An edge-to-face interaction is prevalent in complexes of thrombin with both substrates and inhibitors. Within the aryl-binding pocket of thrombin, the face of the indole side chain of Trp215 is relatively exposed to solvent (Fig. 1) and can serve as the hydrogen-bond acceptor ring in edge-to-face interactions (Fig. 2). For example, the Phe8 aromatic ring of the fibrinogen substrate (Martin *et al.*, 1992), the Tyr3 side chain of the thrombin inhibitor hirudin (Rydel *et al.*, 1990) and the (D)Phe rings of the peptidomimetic inhibitors (D)Phe-Pro-Arg chloromethylketone (PPACK; Bode *et al.*, 1989) and Ac-(D)Phe-Pro-boroArg-OH (DuP714, Weber *et al.*, 1995), all form edge-to-face interactions with Trp215. To utilize this preferred interaction, aromatic ring systems have been incorporated into many synthetic thrombin inhibitors and the existence of the interaction has been confirmed in the crystallographic structures of thrombin complexed with several inhibitors, including sodium [(2-naphthyl sulfonyl)glycyl]-DL-*p*-amidinophenylalanylpiperidide (NAPAP; Brandstetter *et al.*, 1992), a retro-binding peptide inhibitor (Tabernero *et al.*, 1995) and a designed non-peptide inhibitor (Obst *et al.*, 1995).

Structure-based approaches led to the design of [*N*-(3-phenylpropionyl)-*N*-(phenethyl)]-Gly-boroLys-OH, a novel class of thrombin inhibitor (HPBK, Fig. 1, Table 1; Galemmo *et al.*, 1996). The crystal structure of HPBK complexed with thrombin, described here, shows that the phenethyl ring of HPBK forms an edge-to-face interaction with the Trp215 side chain. The tenfold reduction in affinity relative to DuP714 prompted further elaboration of the compound to increase potency and block potential sites of metabolism in the phenethyl group. The structure of the HPBK–thrombin

complex suggested that inhibitor affinity could be enhanced by strengthening the edge-to-face interaction. The perpendicular arrangement of aromatic rings is thought to be stabilized by a favorable electrostatic interaction between the partially positively charged H atoms of the donor ring and the π-electron cloud of the acceptor ring (Fig. 2; Chipot *et al.*, 1996; Jada *et al.*, 1975; Levitt & Perutz, 1988; Pawliszyn *et al.*, 1984). The strength of the edge-to-face interaction is, therefore, expected to vary with the difference in charge between the donor-ring H atoms and the acceptor-ring π-cloud. One strategy to strengthen this interaction involves modification of the donor ring to increase the effective positive charge of its H atoms. Hammett sigma values (σ_H), derived from the changes in ionization of benzoic acid arising from substitutions on the benzene ring, provide a measure of the inductive polarization of aromatic rings (Hammett, 1937). Addition of electron-

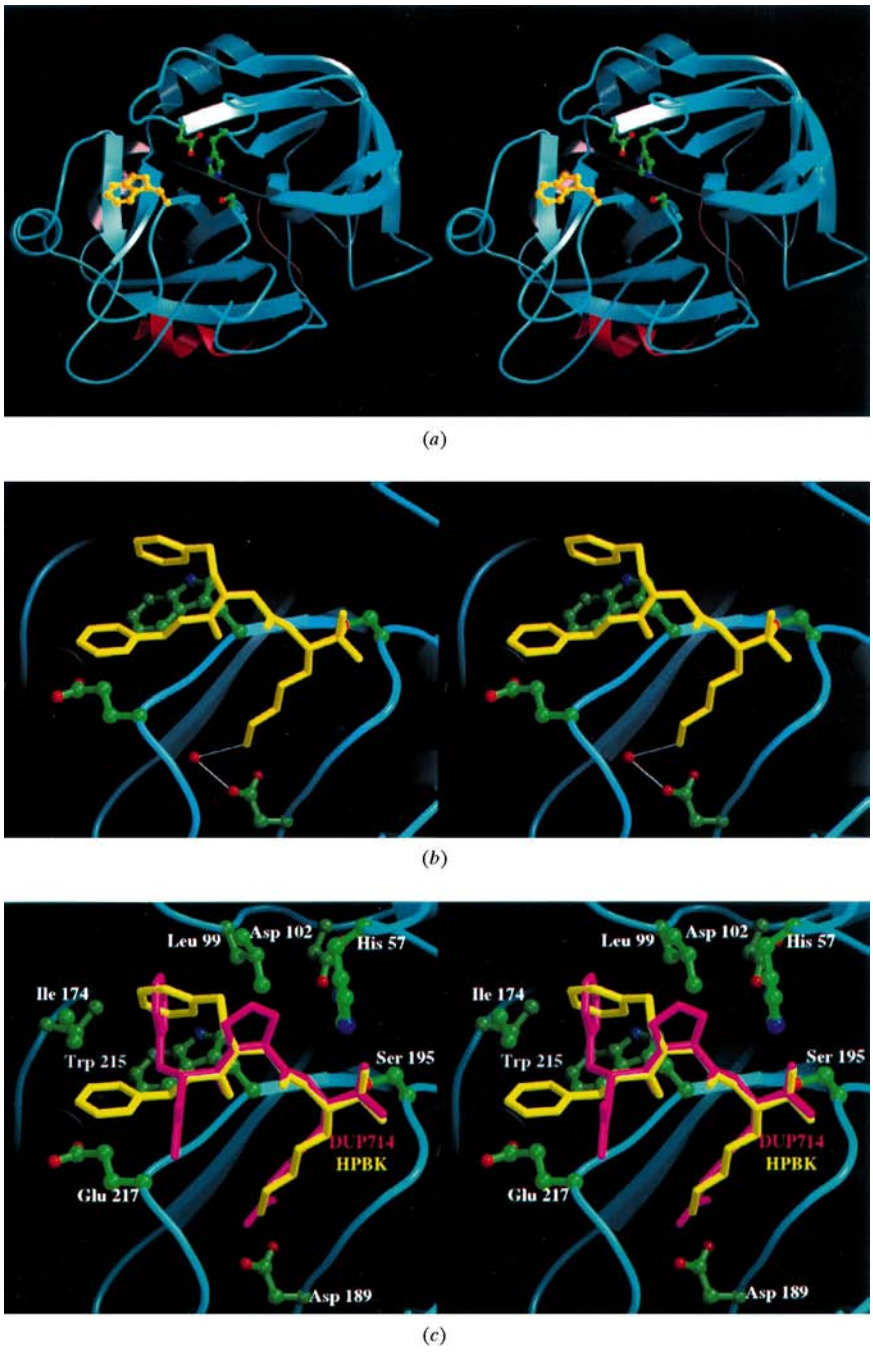

Fig. 1. (*a*) Stereoscopic view of the α-thrombin structure and HPBK binding site. The 26-residue A-chain (red ribbon) and 249-residue B-chain (blue ribbon) are covalently bonded *via* a disulfide bond. The catalytic triad composed of residues His57, Aspl02 and Ser195, is shown in green. The solvent-exposed indole side chain of Trp215 is shown in yellow. (*b*) Enlarged stereoscopic view of HPBK binding site showing the bridging water molecule between the lysine side chain of HPBK and Asp199, the covalent bond between the inhibitor B atom and side-chain O atom of Ser195, packing of the hydrocinnamoyl against Glu217 and the edge-to-face interaction of HPBK with Trp215. (*c*) Stereoviews of thrombin complexed with HPBK (yellow) and DuP714 (Weber *et al.*, 1995; PDB code 1LHC).

Table 1. *Kinetic and crystallographic data for thrombin complexed with HPBK and its 3′ substituted analogs*

R	H	CH_3	CF_3	F	OCH_3
K_i (n*M*)	0.42 ± 0.07	0.20 ± 0.07	0.37 ± 0.13	0.60 ± 0.06	0.91 ± 0.27
σ value†	0.0	−0.06	0.43	0.34	0.11
Resolution range (Å)	8–1.8	8–2.5	8–2.0	8.0–2.3	8.0–2.0
Number of reflections‡	28275	9266	21329	11936	19423
Highest resolution $\langle I/\sigma_I \rangle \geq 2$	<1.8	2.6	<2.0	2.3	2.2
Crystallographic *R* factor (%)	19.6	16.9	18.7	18.4	19.8
Number of atoms§					
Solvent	145	120	130	114	136
Ligand	32	33	36	33	34
R.m.s. coordinate error (Å)¶	0.23	0.23	0.23	0.25	0.24
R.m.s. deviations					
Bond lengths (Å)	0.010	0.016	0.014	0.016	0.011
Bond angles (°)	1.97	1.64	1.73	1.61	1.80
Bond *B* factors††	1.14	1.18	1.20	1.18	1.17
R.m.s. deviations‡‡					
Backbone atoms (Å)	—	0.074	0.031	0.060	0.068
All atoms (Å)	—	0.146	0.335	0.209	0.173

† Values taken from reference (Maskill, 1985) as originally defined by Hammett (1937). ‡ Number of reflections with $I > 0.5I/\sigma_I$. § A-chain residues 1B–14J, B-chain residues 16–146 and 150–245 and hirudin residues 54–60 were used in the refinement of all structures for a total of 2292 protein atoms. ¶ As described by Luzzati (1952). †† $\sum(b_i - b_j)^2/\sigma^2_{\text{bonds}}$. ‡‡ Compared with HPBK–thrombin complex.

withdrawing substituents, having positive σ_H values, increases the relative positive charge of the ring H atoms. Rings containing substituents with positive σ_H values should produce stronger edge-to-face interactions relative to those of an unsubstituted ring. Using a series of small molecules with two gently constrained conformational states, the inductive effect was estimated to increase the stability of an edge-to-face interaction by ~0.5 kcal mol^{-1} (Paliwal *et al.*, 1994).

Here we report the synthesis of phenethyl-substituted HPBK analogs designed to determine the extent to which inhibitor affinity could be modulated by alterations in the strength of the edge-to-face interaction. The structure of the HPBK–thrombin complex revealed a surface pocket large enough to accommodate small substituents at the *meta* position of the phenethyl ring. Methyl ($\sigma_H = -0.06$), methoxy ($\sigma_H = 0.11$), fluoro ($\sigma_H = 0.34$) and trifluoromethyl ($\sigma_H = 0.43$) analogs were synthesized and analyzed. To understand the lack of correlation between substituent σ_H value and observed binding affinity (Fig. 3), crystallographic structures of inhibitors bound to thrombin were determined. As described, two binding modes for the substituted phenethyl group were observed. The protein structure was unchanged by inhibitor binding, although rearrangements in solvent occurred. Overall, these studies provide a demonstration that, in addition to its role in inhibitor design, crystallographic information is critical for understanding binding affinities in situations where the observed data are contrary to hypothesis (Meyer *et al.*, 1995).

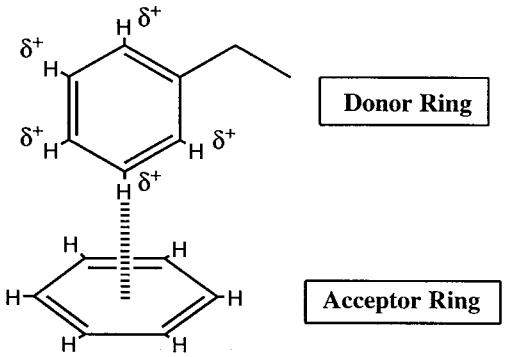

Fig. 2. Schematic diagram of the edge-to-face interaction between aromatic rings.

2. Experimental procedures

2.1. *Chemical synthesis*

The synthesis of HPBK and related borolysine thrombin inhibitors was accomplished in a convergent manner in which an α-amino boronate was coupled to an appropriate *N*,*N*-disubstituted glycine derivative. The optically pure α-amino boronic ester component, (+)-pinanediol (*S*)-1-amino-5-bromopentyl boronate hydrochloride was prepared in five steps from 4-bromo-1-butene using the homologation procedure of Matteson (Matteson *et al.*, 1984). The *N*,*N*-disubstituted glycines were prepared by standard laboratory procedures and coupled with the α-amino boronate using the mixed anhydride method of peptide-bond formation. The bromobutyl side chains were converted to the required lysine side chains *via* azide intermediates (Kettner *et al.*, 1990; Wityak *et al.*, 1995). Finally, the pinanediol esters were removed by transesterification with phenylboric acid to afford the free boronic acid inhibitors as amorphous solids. The identity of all intermediates was supported by spectroscopic methods and the structures of the final compounds, HPBK, trifluoromethyl-HPBK,

fluoro-HPBK, methoxy-HPBK and methyl-HPBK, were confirmed by X-ray crystallographic analysis of their complexes with thrombin.

2.2. *Inhibition studies*

Binding constants of inhibitors for human α-thrombin were determined at 298 K in 0.10 m*M* sodium phosphate buffer pH 7.5 containing 0.20 *M* sodium chloride and 0.5% polyethylene glycol 8000. Assays were conducted with human α-thrombin (with a specific activity of 2340 NIH units mg^{-1}) at a level of 0.2 n*M* and with the chromogenic substrate H-(D)-Phe-Pip-Arg-pNA (S2238). Values of K_i were determined by the methods described previously (Weber *et al.*, 1995). All inhibitors were slow binding. Steady-state velocities were obtained after a reaction time of 25 min with the inhibitor, and the equation for competitive inhibition readily fit the velocities measured. Reported K_i values are the average steady-state values shown with standard deviations for multiple determinations.

2.3. *Crystallization*

A crystal form of thrombin suitable for preparing thrombin–inhibitor complexes in the crystalline state was grown as previously described (Skrzypczak-Jankun *et al.*, 1991). Crystals belong to the monoclinic space group *C*2 (a = 70.7, b = 72.3, c = 72.5 Å and β = 100.4°) and contain one molecule per crystallographic asymmetric unit. To prepare the thrombin–inhibitor complex, 1 mg of inhibitor was dissolved in 10 µl of DMSO, then added to 250 µl of crystal stabilization solution (0.058 *M* sodium phosphate pH 7.2, 33% polyethylene glycol 8000, 0.05 m*M* NaN_3) containing 1–2 crystals. Crystals were soaked with inhibitor for at least 48 h prior to data collection.

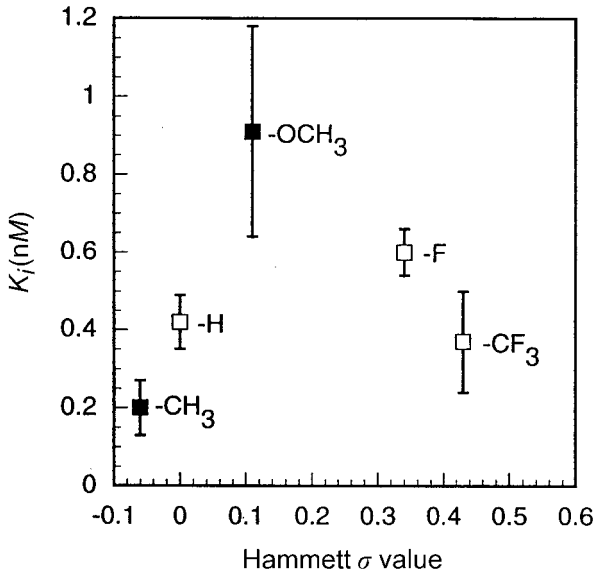

Fig. 3. Plot of inhibition constant (K_i) *versus* Hammett α value. Inhibitors retaining the edge-to-face interaction are denoted by open boxes, others by filled boxes.

2.4. *Data collection*

Data were collected with a Rigaku R-AXIS IIC image-plate detector system mounted on a Rigaku RU-200B rotating-anode X-ray generator (100 mA, 50 kV) with a 0.3 × 0.3 mm focus. X-ray diffraction intensities were collected at room temperature in 60 contiguous 2° oscillations counted for 30 min each. Crystals were sufficiently stable in the X-ray beam to allow use of one crystal for a complete data set. Diffraction data were reduced to integrated intensities using software provided with the Rigaku R-AXIS IIC image-plate detector or with the programs *XDISPLAYF*, *DENZO* and *SCALEPACK* (Otwinowski & Minor, 1997). Data-collection statistics for the various complexes are summarized in Table 1.

2.5. *Structure solution and refinement*

Coordinates of thrombin, taken from the 1.95 Å resolution DuP714–thrombin complex (Weber *et al.*, 1995), were used as the starting model for refinement of the thrombin–HPBK complex. The thrombin coordinates refined with bound HPBK were then used as the starting structure for each of the substituted HPBK–thrombin complexes. Each cycle of refinement (*X-PLOR* version 3.1; Brünger *et al.*, 1987) consisted of 50 cycles of conjugate-gradient minimization, followed by 20 cycles of restrained individual *B*-factor refinement, followed by a further 20 cycles of conjugate-gradient minimization and finished with ten additional cycles of

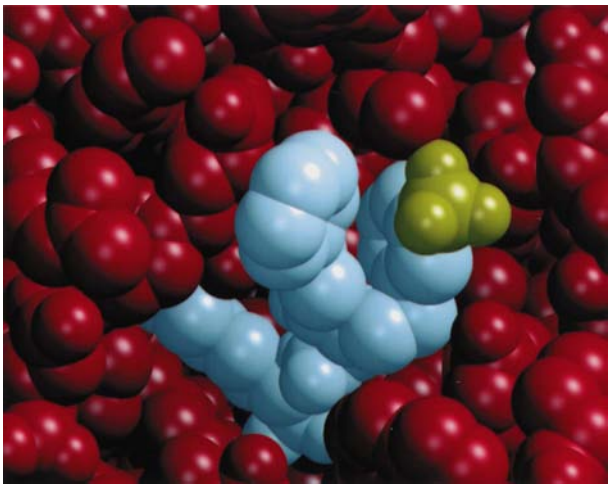

Fig. 4. Hypothesis for addition of *meta* substituents. The van der Waals surfaces of the thrombin active-site cleft and aryl-binding pocket are red. The van der Waals surface of the bound HPBK is shown in white. A 3′-trifluoromethyl group attached to the phenethyl ring of HPBK (shown in yellow) can be accommodated within the aryl-binding pocket without alteration of thrombin structure.

B-factor refinement. After each refinement cycle, the model was manually adjusted based upon interpretation of $(F_o - F_c)\alpha_{\rm calc}$ and $2(F_o - F_c)\alpha_{\rm calc}$ electron-density maps displayed with the computer graphics program *CHAIN* (Sack, 1988). Potential water-molecule positions were initially located as 3σ positive peaks in the $(F_o - F_c)\alpha_{\rm calc}$ electron-density map with corresponding 0.8σ positive peaks in $2(F_o - Fc)\alpha_{\rm calc}$ electron-density maps. Positions satisfying these positive density criteria were added to the atomic model if reasonable hydrogen-bond geometry to thrombin could be established. Inhibitor geometric and atomic refinement parameters were calculated using the program *QUANTA* (Molecular Simulations Inc.). Refinement statistics for the thrombin–inhibitor complexes are listed in Table 1.

3. Results

Interactions of HPBK with thrombin HPBK, a peptidomimetic of the thrombin substrate sequence Gly-Pro-Arg-Gly, incorporates a boronic acid group which, on complexation with thrombin, forms a covalent bond with the active-site serine. In the covalent complex, the boron adopts a tetrahedral geometry resembling the transition state of serine proteases (Kraut, 1977). Overall, HPBK retains many of the binding features of the previously described peptidomimetic thrombin inhibitors PPACK (Bode *et al.*, 1989) and DuP714 (Fig. 1; Weber *et al.*, 1995). For example, the HPBK lysine side chain occupies the thrombin S1 specificity pocket and interacts with Asp189 *via* a bridging water molecule. Similar to the substrate and peptide-based inhibitors, the carbonyl O atom of the hydrocinnamoyl group forms a hydrogen bond with the main-chain N atom of Gly216 and the backbone amide N atom of the borolysine is hydrogen bonded to the carbonyl backbone of Ser214. The phenyl ring packs against the alkyl chain of Glu217.

The phenethyl aromatic ring of HPBK is situated in the aryl pocket and forms an aromatic edge-to-face interaction with Trp215 (Fig. 1). The 5.3 Å centroid-to-centroid distance between the two rings and 70° inter-ring angle are similar to values reported for tryptophan edge-to-face interactions with phenylalanine in protein structures (Burley & Petsko, 1985) where an average 5.9 Å centroid-to-centroid distance and 60° inter-ring angle were found.

The *meta* position of the phenethyl ring is relatively exposed to solvent (Fig. 4) with two ordered solvent molecules, Wat1 and Wat2, nearby (Fig. 5). Wat1 is hydrogen bonded both to the backbone carbonyl group of Trp96 and the OH group of Tyr60A. The more weakly bound water molecule, Wat2, forms a 3.0 Å hydrogen bond to the backbone carbonyl group of Glu97A. A van der Waals surface representation of the HPBK–thrombin complex (Fig. 4) suggested that groups as large as trifluoromethyl could be accommodated at the *meta* position of the phenethyl ring without steric hindrance by protein atoms.

3.1. *Binding constants of inhibitors*

Thrombin inhibition constants for HPBK and its analogs are given in Table 1. HPBK binds thrombin with a K_i of 0.42 n*M*. The trifluoromethyl analog binds with comparable affinity, while the fluoro and methoxy analogs exhibit decreased affinity relative to HPBK (K_i = 0.60 and 0.91 n*M*, respectively). Only methyl-HPBK binds more tightly (K_i = 0.20 n*M*).

3.2. *Binding of 3′-substituted HPBK analogs*

The bound conformations of HPBK and its analogs are crystallographically well defined. Continuous density is seen for each of the inhibitors and the position of the *meta* substituent is unambiguous (Fig. 6). Little variation in the structure of thrombin is observed. The r.m.s. differences in thrombin backbone atom coordinates for the various complexes is less than 0.1 Å (Table 1). In most aspects, the substituted HPBK derivatives bind the same as HPBK. Both the lysine side chain-to-aspartic acid interaction in the S1 specificity pocket and the hydrogen bonding between inhibitor amide and carbonyl groups and thrombin main-chain atoms are present.

Despite an overall preservation of many key interactions, the inhibitor phenethyl ring binds either with retention of the edge-to-face interaction or rotates so that the *meta* substituent interacts directly with Trp215 (Fig. 7). The position of Wat2, as described below, varies with orientation of the phenethyl ring (Fig. 5).

The phenethyl ring of three inhibitors, HPBK and its fluoro and trifluoromethyl analogs, forms an edge-to-face interaction with Trp215 (Fig. 5). For these compounds, the geometric parameters of the edge-to-face interaction are similar (Fig. 7). Distances between the centroid of Trp215 and the phenethyl ring are 5.3, 5.4 and 5.3 Å for fluoro-HPBK, trifluoromethyl-HPBK and HPBK, respectively. Similar inter-ring angles are also observed (68, 62 and 70° for fluoro-HPBK, trifluoromethyl-HPBK and HPBK, respectively). The 8° difference in inter-ring angle for trifluoromethyl-HPBK is due to formation of a water-mediated hydrogen bond between a fluorine of the inhibitor and the backbone carbonyl of Glu97A. Inclusion of Wat2 in this bonding pattern results in a 1 Å positional shift and a 0.3 Å increase in the length of its hydrogen bond with Glu97A (Fig. 5*e*). A similar fluorine–water–backbone carbonyl hydrogen bond is observed for fluoro-HPBK, although in this complex no significant movement of Wat2 occurs.

The X-ray crystallographic structures of the thrombin methyl– and methoxy–HPBK complexes showed that no edge-to-face interaction with Trp215 occurred on binding (Fig. 5). Instead the phenethyl ring rotated

~135° relative to HPBK, so that the 3′ substituent interacted directly with Trp215. Greater rotation of the phenethyl ring is prevented by the approach of the *ortho* C atom to within 3.3 Å of the hydroxyl group of Tyr60A. Larger phenethyl ring to Trp215 indole distances of 6.0 and 6.4 Å are observed for the thrombin methyl- and methoxy-HPBK complexes, respectively. The methyl groups are within 3.7 and 3.2 Å of the Trp215 indole for the methyl- and methoxy-HPBK inhibitors, respectively. The positions of Wat1 and Wat2 are unaffected by inhibitor binding.

4. Discussion

Having observed a specific edge-to-face interaction in the thrombin–HPBK complex, a strategy to modulate its strength was tested by the synthesis of four HPBK analogs (Galemmo *et al.*, 1996). Crystallographic and kinetic analyses of these compounds binding to α-thrombin show that the edge-to-face interaction can be weakly modulated by through-ring inductive effects. For example, the phenethyl groups of both fluoro-HPBK and trifluoromethyl-HPBK form an edge-to-face

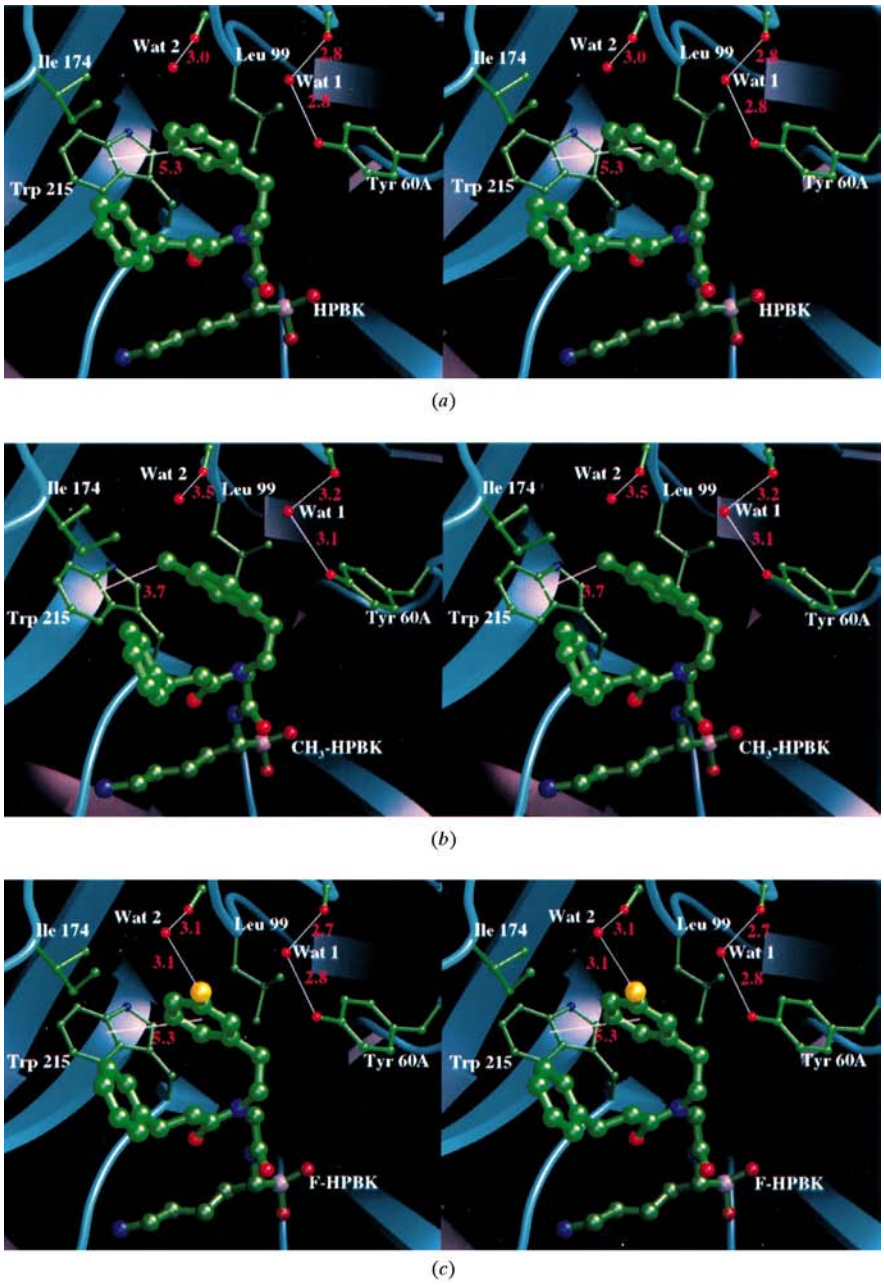

Fig. 5. Details of interaction between thrombin and HPBK series of inhibitors shown as stereoviews. Distances between interacting groups are given in Å. (*a*) HPBK, (*b*) methyl-HPBK, (*c*) fluoro-HPBK, (*d*) methoxy-HPBK, (*e*) trifluoromethyl-HPBK. When the 145 immobilized solvent molecules found in the HPBK–thrombin complex are ordered by electron-density value in the final $2(F_o - F_c)\alpha_{calc}$ electron-density map, Wat1 (B value = 33 Å^2) ranks 51st and Wat2 (B value = 45 Å^2) 101st.

interaction with the indole side chain of Trp215 within the thrombin aryl-binding pocket. The F atoms of the 3′-phenethyl substituent form hydrogen bonds with an immobilized water molecule which, in turn, is hydrogen bonded to the backbone carbonyl O atom of Glu97A. For these homologous compounds making very similar interactions with thrombin, the observed higher affinity of trifluoromethyl-HPBK (K_i = 0.37 n*M*) relative to fluoro-HPBK (K_i = 0.60 n*M*) is likely to be a reflection of the greater electron-withdrawing effects of CF_3 (α_H = 0.43) compared with F (α_H = 0.34). Minor changes in affinity are consistent with previous studies showing that the edge-to-face interaction itself is relatively weak (Adams *et al.*, 1996; Jada *et al.*, 1975; Paliwal *et al.*, 1994).

Comparison of the bound conformations of HPBK and methyl-HPBK suggests that the edge-to-face interaction, albeit somewhat destabilized by addition of the 3′ methyl group (α_H = 0.0 for H and −0.06 for CH_3), is weaker than the interaction between the phenethyl methyl group and the π-cloud of the Trp215 side chain. Semiempirical calculations (*INSIGHT*, Molecular Simulations Inc.) indicate that H atoms of a methyl group attached to an aromatic ring and the phenyl H atoms have approximately the same partial charge. The higher affinity of the methyl-HPBK analog may reflect the packing of two partially charged H atoms near the Trp215 indole side chain, instead of one which would be the case if the phenethyl and Trp215 rings formed an edge-to-face interaction.

The structural data provide evidence that both the edge-to-face and methyl-to-aromatic interactions are specific and somewhat directional. Within the phenethyl side chain, lower *B* values for atoms directly interacting with the Trp215 indole are observed. For fluoro-HPBK and trifluoromethyl-HPBK, where the edge-to-face interaction is preserved, the average *B* values for the phenyl ring atoms are 34 and 35 Å^2, while the average *B* values of the 3′ substituents are 38 and 43 Å^2, respectively. Similarly, the methyl substituent of methyl-HPBK which packs adjacent to the indole ring is immobilized to a greater extent than the phenyl ring, *i.e.* the average *B* values for the phenyl ring atoms and methyl group are 16 and 13 Å^2, respectively.

The lower affinity of the 3′-methoxy analog may reflect binding of a substituted aromatic side chain whose overall size and shape are not ideal for the aryl-binding pocket of thrombin. Several close contacts within this complex are observed. These include a 3.2 Å separation between the methoxy methyl group and the centroid of the Trp215 indole and a 3.1 Å separation between phenethyl ring C atom and hydroxyl side chain

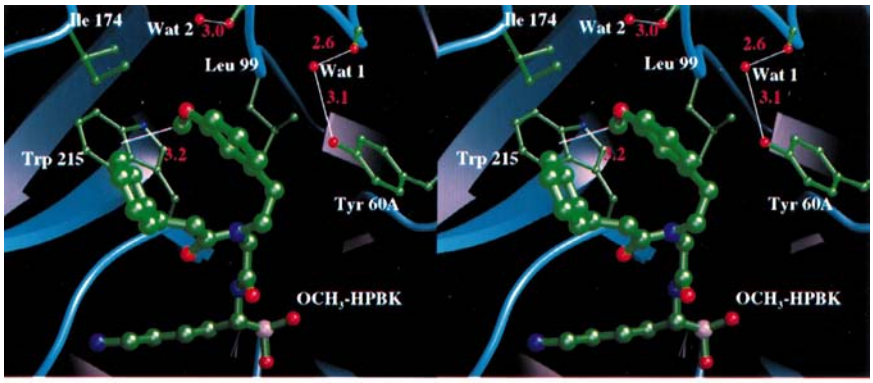

(*d*)

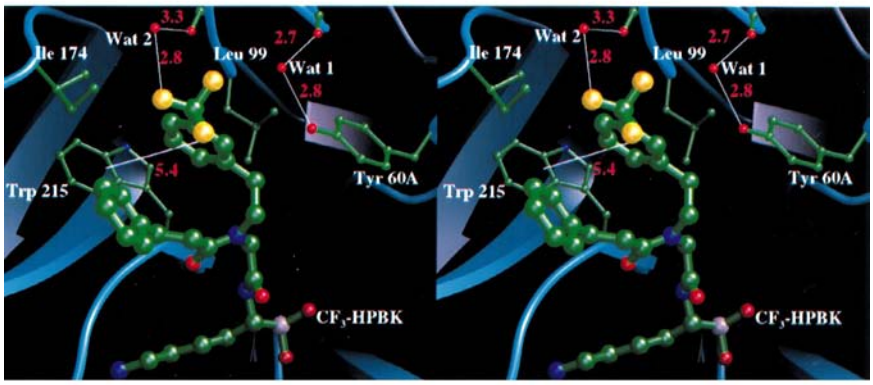

(*e*)

Fig. 5 (*cont.*)

of Tyr60A. Unlike the fluoro-, trifluoromethyl- and methyl-HPBK analogs, little variation in *B* value for the phenethyl side chain is seen in the 3′-methoxy HPBK–thrombin complex. For this compound, the average *B* value for the phenyl ring atoms is 45 Å^2 and the average *B* value of the 3′-substituent atoms is 44 Å^2. Lack of variability in side-chain *B* value again indicates the inability of the 3′-methoxy phenethyl group to optimally pack within the aryl-binding pocket.

Two methods for increasing the binding affinity of compounds whose substituents participate in edge-to-face interactions are demonstrated here. Either approach, addition of electron-withdrawing substituents to increase the strength of the edge-to-face interaction or addition of substituents to directly interact with the acceptor aromatic system, may find general utility in drug design. Such substitutions may be particularly well suited for thrombin inhibitors where an edge-to-face interaction involving the indole side chain of Trp 215 is frequently observed.

Overall, these studies demonstrate how weak interactions determine the equilibrium conformation of molecules bound to proteins. Systematic studies of single types of interactions, such as those described here, will assist in understanding the relative contributions of these forces within the complex environment of solvated proteins.

We thank F. Lewandowski and L. Mersinger for technical assistance.

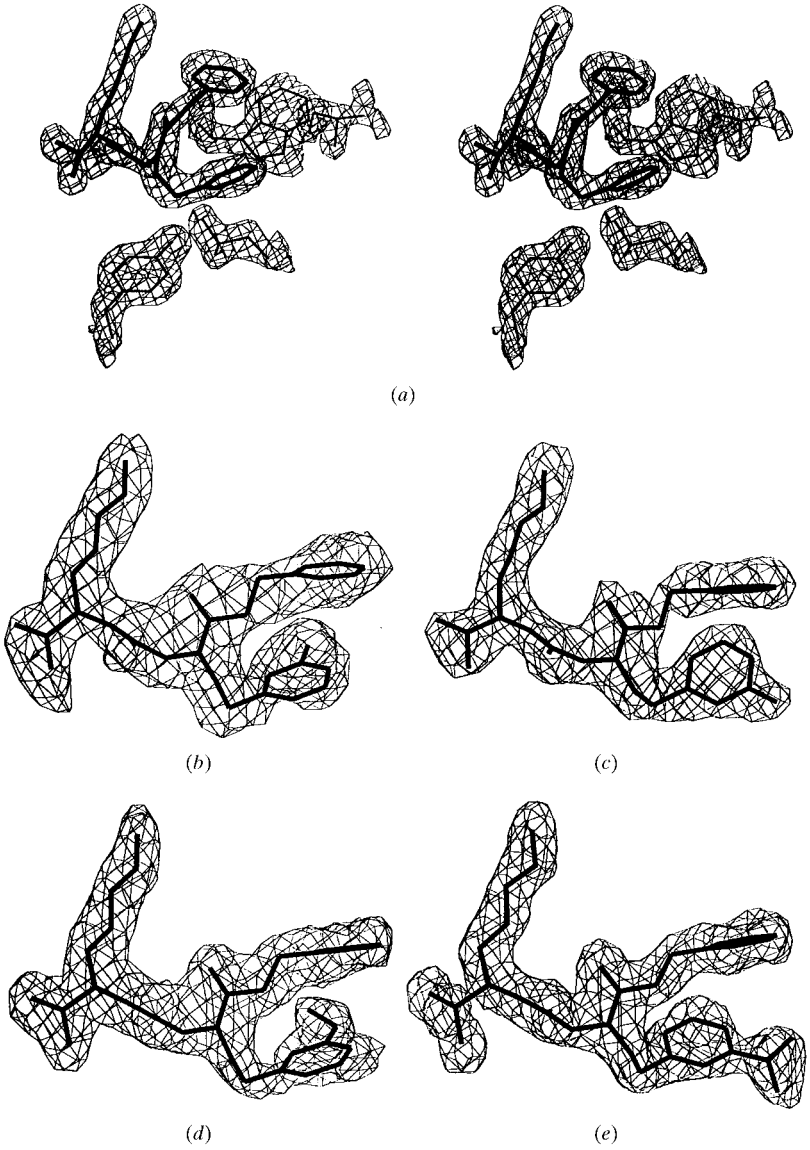

Fig. 6. Electron density for HPBK and its *meta*-substituted analogs. (*a*) Stereoscopic views of HPBK $(2F_o - F_c)\alpha_{calc}$ electron density contoured at 1.6σ. (*b*) Methyl-HPBK $(2F_o - F_c)\alpha_{calc}$ electron-density map contoured at 0.7σ. (*c*) Fluoro-HPBK $(2F_o - F_c)\alpha_{calc}$ electron-density map contoured at 1.1σ. (*d*) Methoxy-HPBK $(2F_o - F_c)\alpha_{calc}$ electron-density map contoured at 0.8σ. (*e*) Trifluoromethyl-HPBK $(2F_o - F_c)\alpha_{calc}$ electron-density map contoured at 1.0σ.

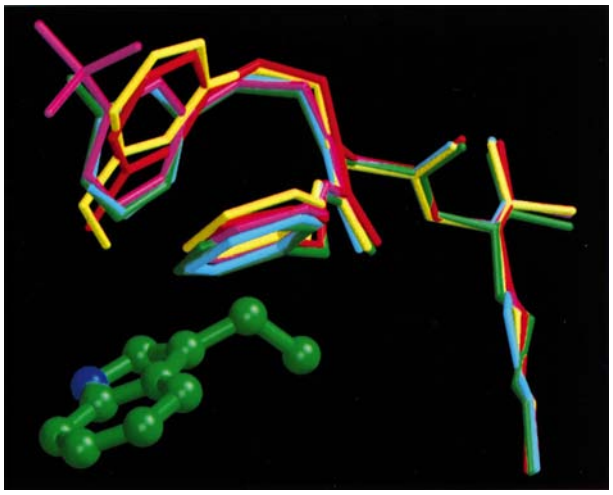

Fig. 7. Overlay of HPBK derivatives showing their interaction with Trp215. HPBK, blue; methyl-HPBK, red; fluoro-HPBK, green; methoxy-HPBK, yellow; trifluoromethyl-HPBK, purple.

References

Adams, H., Carver, F., Hunter, C., Morales, J. & Seward, E. (1996). *Angew. Chem. Int. Ed. Engl.* **35**, 1542–1544.

Bode, W., Mayr, I., Baumann, U., Huber, R., Stone, S. & Hofsteenge, J. (1989). *EMBO J.* **8**, 3467–3475.

Brandstetter, H., Turk, D., Hoeffken, H., Grosse, D., Stuerzebecher, J., Martin, P., Edwards, B. & Bode, W. (1992). *J. Mol. Biol.* **226**, 1085–1099.

Brünger, A., Kuriyan, J. & Karplus, M. (1987). *Science*, **235**, 458–460.

Burley, S., Wang, A., Votano, J. & Rich, A. (1987). *Biochemistry*, **26**, 5091–5099.

Burley, S. K. & Petsko, G. A. (1985). *Science*, **229**, 23–28.

Chipot, C., Jaffe, R., Maigret, B., Pearlman, D. & Kollman, P. (1996). *J. Am. Chem. Soc.* **118**, 11217–11224.

De Vos, A., Tong, L., Milburn, M., Matias, P., Jancarik, J., Noguchi, S., Nishimura, S., Miura, K., Ohtsuka, E. & Kim, S. (1988). *Science*, **239**, 888–893.

Galemmo, R., Fevig, J., Carini, D., Cacciola, J., Wells, B., Hillyer, G., Buriak, J., Rossi, K., Stouten, P., Alexander, R., Hilmer, R., Bostrom, L., Abelman, M., Lee, S., Weber, P., Kettner, C., Knabb, R. & Wexler, R. (1996). *Bioorg. Med. Chem. Lett.* **6**, 2913–2918.

Hammett, L. (1937). *J. Am. Chem. Soc.* **59**, 96–103.

Hunter, C., Singh, J. & Thornton, J. (1991). *J. Mol. Biol.* **278**, 837–846.

Ishida, T., Tarui, M., In, Y., Ogiyama, M., Doi, M. & Inoue, M. (1993). *FEBS Lett.* **33**, 214–216.

Jada, K., Hemminger, J., Winn, J., Novick, S., Harris, S. & Kemplerer, W. (1975). *J. Chem. Phys.* **63**, 1419–1421.

Kettner, C., Mersinger, L. & Knabb, R. (1990). *J. Biol Chem.* **265**, 18289–18297.

Kraut, J. (1977). *Annu. Rev. Biochem.* **46**, 331–358.

Levitt, M. & Perutz, M. (1988). *J. Mol. Biol.* **201**, 751–754.

Luzzati, P. (1952). *Acta Cryst.* **5**, 802–810.

Martin, P., Roberts, W., Turk, D., Huber, R., Bode, W. & Edwards, B. (1992). *J. Biol. Chem.* **267**, 7911–7920.

Maskill, H. (1985). *The Physical Basis of Organic Chemistry.* New York: Oxford University Press.

Matteson, D., Jesthi, P. & Sadhu, K. (1984). *Organometallics*, **3**, 1284–1288.

Meyer, E. F., Botos, I., Scapozza, L. & Zhang, D. (1995). *Perspect. Drug Discovery Des.* **3**, 168–195.

Obst, U., Gramlich, V., Diederich, F., Weber, L. & Banner, D. (1995). *Angew. Chem. Int. Ed. Engl.* **34**, 1739.

Otwinowski, Z. & Minor, W. (1997). *Methods Enzymol.* **276**, 306–326.

Paliwal, S., Geib, S. & Wilcox, C. (1994). *J. Am. Chem. Soc.* **116**, 4497–4498.

Pawliszyn, J., Szczesniak, M. & Scheiner, S. (1984). *J. Chem. Phys.* **63**, 1419–1421.

Rydel, T., Ravichandran, K., Tulinsky, A., Bode, W., Huber, R., Roitsch, C. & Fenton, J. (1990). *Science*, **249**, 277–280.

Sack, J. (1988). *J. Mol. Graph.* **6**, 224–225.

Singh, J. & Thornton, J. (1985). *FEBS Lett.* **191**, 1–6.

Skrzypczak-Jankun, E., Carperos, V., Ravichandran, K., Tulinsky, A., Westbrook, M. & Maraganore, J. (1991). *J. Mol. Biol.* **221**, 1379–1394.

Tabemero, L., Chang, C., Ohringer, S., Lau, W., Iwanowicz, E., Han, W., Wang, T., Seiler, S., Roberts, D. & Sack, J. (1995). *J. Mol. Biol.* **246**, 14–20.

Weber, P., Lee, S., Lewandowski, F., Schadt, M., Chang, C., & Kettner, C. (1995). *Biochemistry*, **34**, 3750–3757.

Wityak, J., Earl, R., Abelman, M., Bethel, Y., Fisher, B., Kauffman, G., Kettner, C., Ma, P., McMillan, J., Mersinger, L., Pesti, J., Pierce, M., Rankin, F., Chorvat, R. & Confalone, P. (1995). *J. Org. Chem.* **60**, 3717–3722.